Supplementary information

Hydrothermal conversion of cerium oxalate to CeO_2: A parade of oxalate and water coordination modes

Navid Assi [a], Christophe Lahoud [b], Petr Brázda [c], Dominika Zákutná [a], Daniel N. Rainer [d], Jakub Hraníček [e], Jan Rohlíček [c] and Václav Tyrpekl*[,a]

[a] *Department of Inorganic Chemistry, Faculty of Science, Charles University, Hlavova, 2030/8, 12800 Prague, Czech Republic. E-mail: vaclav.tyrpekl@natur.cuni.cz*

[b] *Université Aix-Marseille, Faculty of Science, Site St. Jérôme, 52 Avenue Escadrille Normandie Niemen, 13013 Marseille, France.*

[c] *Department of Structure Analysis, Institute of Physics of the Czech Academy of Sciences, 18221 Prague, Czech Republic*

[d] *Department of Physical and Macromolecular Chemistry, Faculty of Science, Charles University, Hlavova, 2030/8, 12800 Prague, Czech Republic.*

[e] *Department of Analytical Chemistry, Faculty of Science, Charles University, Hlavova, 2030/8, 12800 Prague, Czech Republic*

Synthesis

The starting $Ce_2(C_2O_4)_3·10H_2O$ powder was synthetised according to previously published procedure[10] and solid solution of Ce-Gd oxalates according to work[1]. Solution of oxalic acid (Alfa Aesar 99.5%) was added dropwise into stirred cerium nitrate solution (Alfa Aesar, 99.99%) both having concentration of 0.1 M at room temperature and left 30 min for digestion. The fresh precipitate was purified by centrifugation and dried at 50 °C under air. An analogous procedure was used for Ce-Gd mixed samples ($Gd(NO_3)_3·6H_2O$, Alfa Aesar, 99.99%), only the metal nitrates we mixed in desired molar ratios (10, 20 and 30 mol. % of Gd(III) in the mixture) prior to the precipitation.

The acid solutions were prepared from stock nitric acid (Lach-Ner, 65%), hydrochloric acid (PENTA, 35%) and perchloric acid (Riedel-de Haën, 70%). All the hydrothermal reactions we conducted in 50-mL Teflon autoclave. Final powders were washed with repeated centrifugation and dried at 50 °C under air.

Characterisation methods

Powder X-ray diffraction was recorded on a PANalytical X'Pert PRO diffractometer (Cu Kα radiation). High-temperature patterns were obtained using an Anton-Paar heating cell (HTK 16N, TCU 2000 temperature control unit).

Thermogravimetric analyses were performed on a SETYS Evolution thermogravimeter from SETARAM. The sample was heated from room temperature, with a 20-min delay at 40°C for drying, with a slope of 3 K/min to 800°C in a 100-µl alumina crucible.

The infrared spectra were recorded on Thermo Scientific Nicolet 6700 FTIR with a resolution of 4 cm^{-1}.

The powder morphology was studied using scanning electron microscope JEOL JSM-6510.

Transmission electron microscopy (TEM) and scanning TEM imaging as well as EDS elemental maps were acquired using a JEOL NEOARM 200F atomic resolution analytical electron microscope operating at 200 kV. EDS spectra were obtained with a JEOL JED-2300 EDS spectrometer. The powder samples were deposited on a holey carbon coated copper TEM grid (300 mesh). EDS measurements were conducted for 15 minutes.

3D Electron diffraction (3D ED) experiments were performed on a FEI Tecnai G2 20 microscope (200 kV, λ = 0.0251 Å) with an LaB$_6$ cathode equipped with a Cheetah ASI direct detection camera (16 bit). The temperature of measurement was 150 K (sample holder tip temperature). Data were measured using continuous rotation method with rotation semi-angle of 0.15 or 0.25°. The powder was ground using mortar and pestle. The powder was dispersed in distilled water and deposited on the TEM grid (Cu Quantifoil R 1.2/1.3). Data were processed with PETS2. Optical distortions were compensated using calibrated values. The camera length was calibrated using external standard (lutetium aluminum garnet). The structures were solved using Superflip program and refined in Jana2020/Dyngo using dynamical refinement and the concept of the overlapping virtual frames. In this work we solved 114 datasets.

For composition determination ca. 60-80 mg of the sample was mixed with 2.0 mL of HNO$_3$, 6.0 mL of HCl, 2.0 mL of HF in a Teflon vessel (DAP-60) and digested in Microwave Digestion System (Speedwave Xpert, Berghof Products, Germany). After cooling down, the complexation of the surplus HF was done by adding 12 mL of concentrated H 3 BO 3 solution. After digestion, the solutions were quantitatively transferred into 50 mL polypropylene tubes and diluted for analysis. The chemical composition of prepared GdCe samples was determined by Inductively Coupled Plasma Mass Spectrometry (ICP-MS) measurements (Agilent 7900 ICP-MS; Agilent Technologies, Inc., USA). Ce and Ge were measured at m/z 140 and 157, respectively, in both no gas and helium collision mode (4.3 mL min −1 He) in a collision cell. For sensitivity correction, the sample/standard was mixed with a solution containing 50 µg.L^{-1} terbium (Tb) in 1% HNO$_3$ used as internal standard. The results were obtained using Agilent Mass Hunter software. All samples were measured in triplicates. In all cases, the relative standard deviation was lower than 8 %.

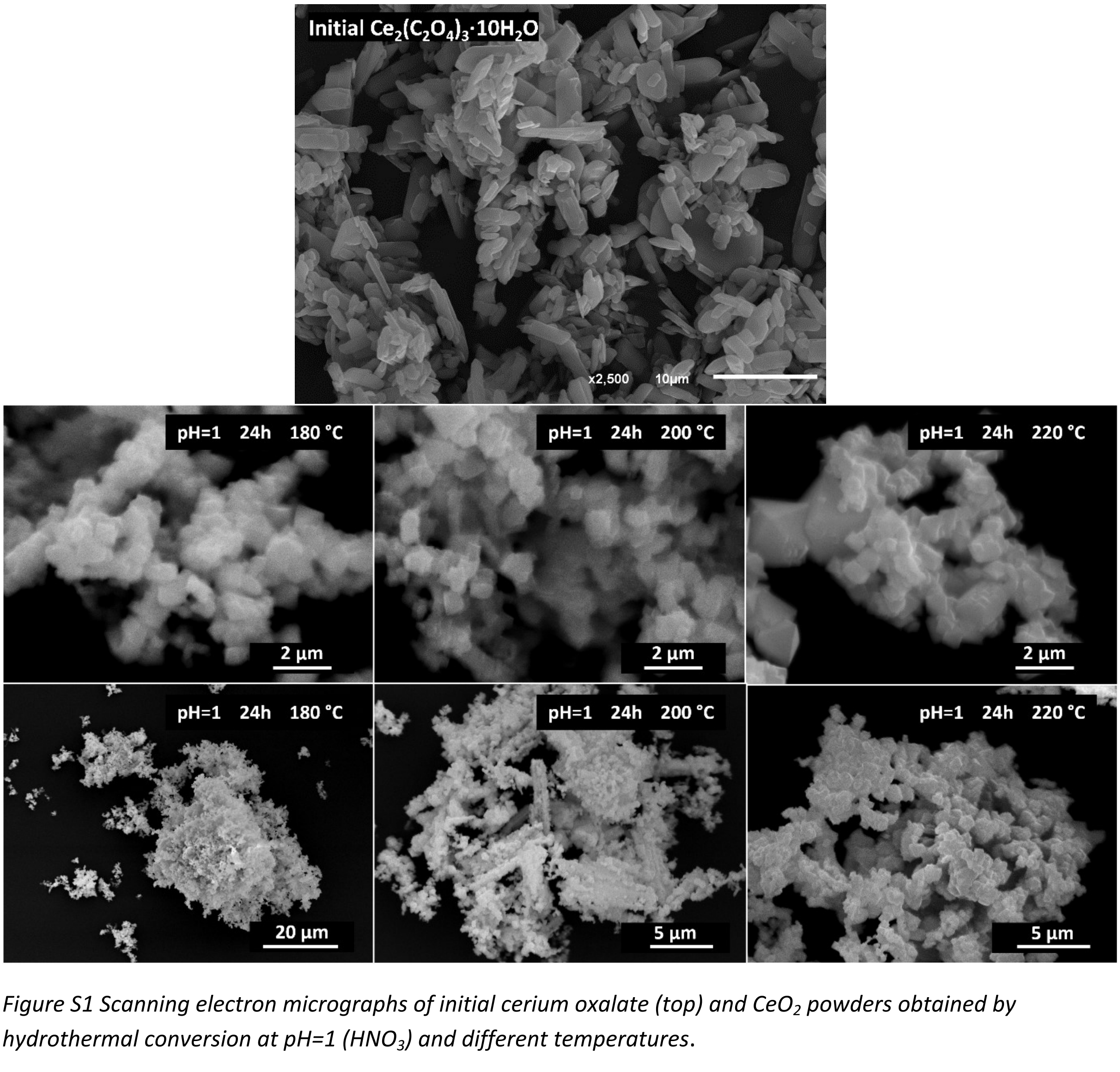

Figure S1 Scanning electron micrographs of initial cerium oxalate (top) and CeO$_2$ powders obtained by hydrothermal conversion at pH=1 (HNO$_3$) and different temperatures.

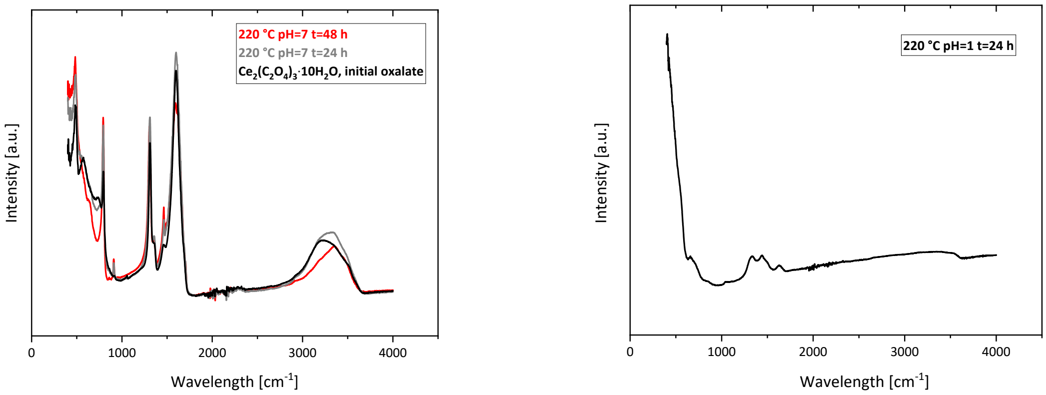

Figure S2 Infrared spectra of initial cerium oxalate and recrystallized and fully converted CeO_2 samples, shoving the oxalate decomposition to oxide.

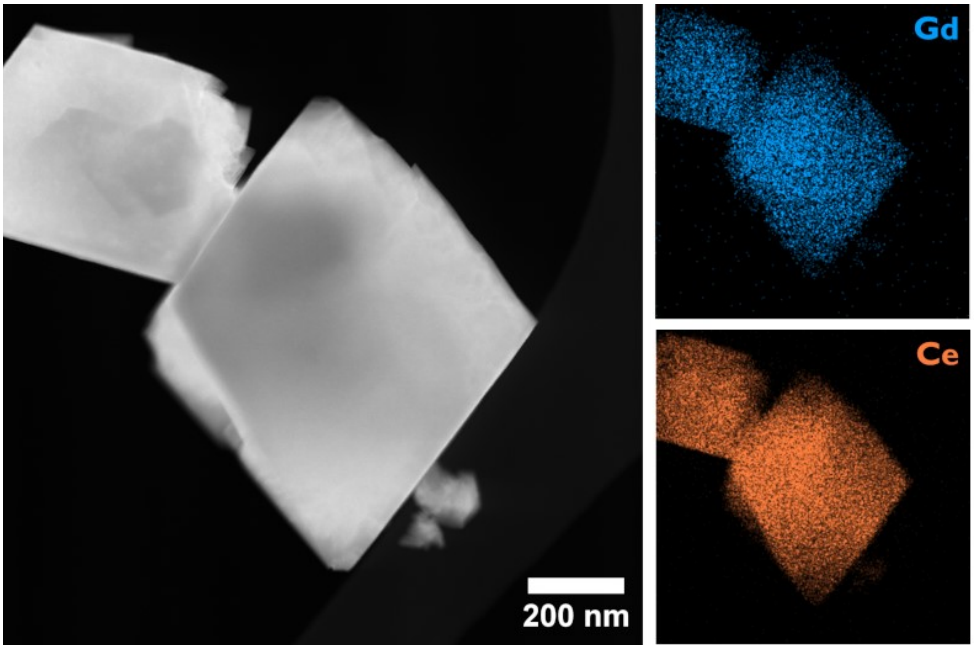

Figure S3 Scanning transmission electron micrograph of mixed $Ce_{1-x}Gd_xO_{2-x/2}$ powder with EDS mapping proving the homogeneity of the sample.

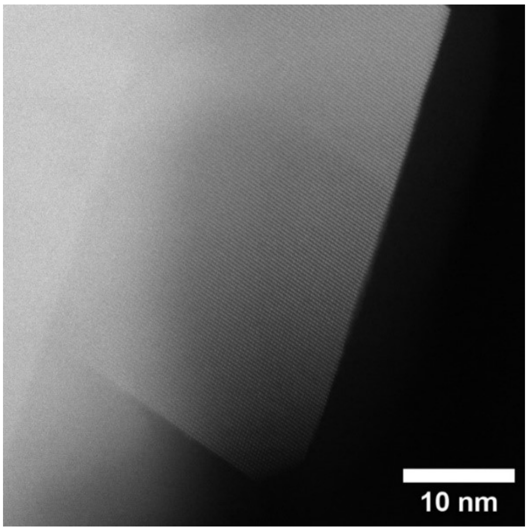

Figure S4 High resolution scanning transmission electron micrograph of $Ce_{0.7}Gd_{0.3}O_{1.85}$ powder/

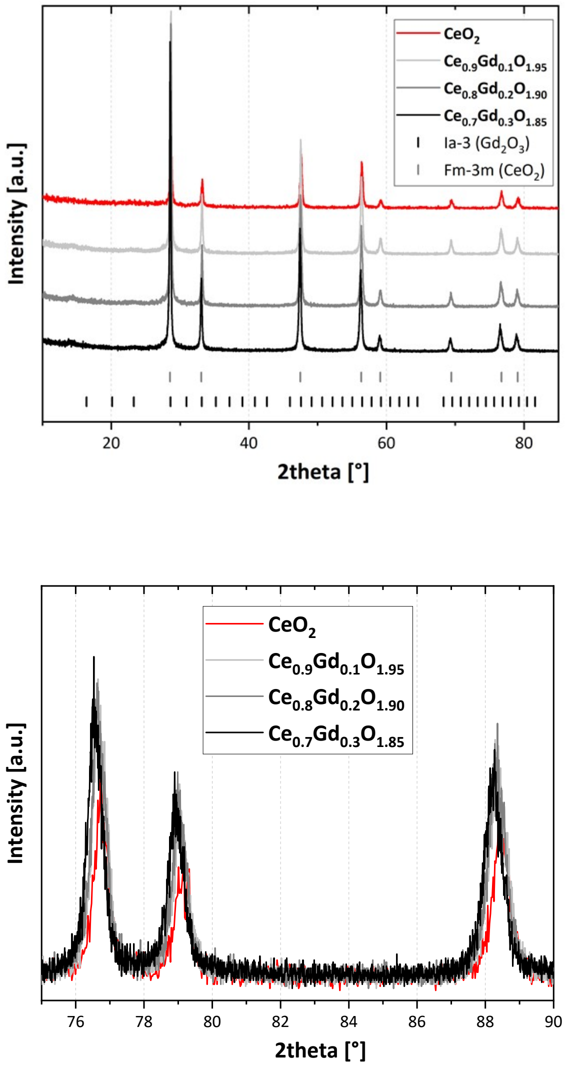

Figure S5 Powder Xray diffraction of $Ce_{1-x}Gd_xO_{2-x/2}$ samples obtained at 220 C, pH=1, 24 hours, overview (top), detail at high 2θ diffractions (bottom), marked with targeted composition of the original mixed oxalate.

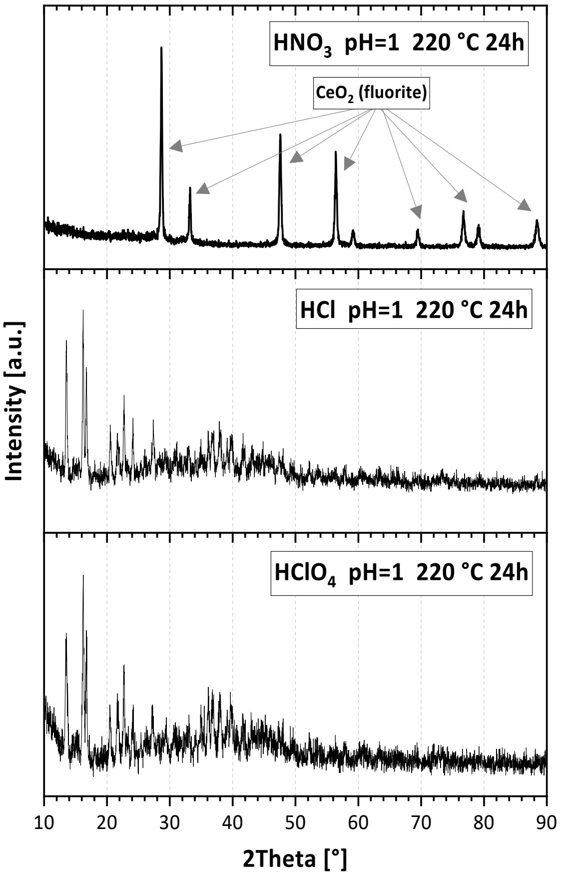

Figure S6 X-ray powder diffraction of cerium oxalate hydrothermally treated at different conditions, nitric acid solution, pH=1, 220 °C for 24 hours (top); the same conditions in hydrochloric acid solution (middle); the same conditions in perchloric acid solution (bottom).

Table S1 Compositions of $Ce_{1-x}Gd_xO_{2-x/2}$ *samples obtained at 220 C, pH=1, 24 hours by ICP-MS.*

Target sample composition	Composition by ICP MS
$Ce_{0.9}Gd_{0.1}O_{1.95}$	$Ce_{0.895}Gd_{0.105}O_{1.85}$
$Ce_{0.8}Gd_{0.2}O_{1.90}$	$Ce_{0.840}Gd_{0.160}O_{1.90}$
$Ce_{0.7}Gd_{0.3}O_{1.85}$	$Ce_{0.733}Gd_{0.267}O_{1.85}$

Table S2 Crystallographic characterisation of phases by 3D electron diffraction (sample treated at 220 °C and 24 hours).

Stoichiometric formula	$Ce_2(C_2O_4)_3(H_2O)_4$	$Ce_2(C_2O_4)_3(H_2O)_4 \cdot H_2O$	$Ce_2(C_2O_4)_3(H_2O)_4 \cdot H_2O$	$Ce_2(C_2O_4)_3(H_2O)_4 \cdot H_2O$
Statistical occurrence (% of cases)	40	39	14	7
Crystal system	Orthorhombic	Triclinic	Orthorhombic	Monoclinic
Space group	$P2_12_12_1$	P-1	*Pbcn*	$P2_1/n$
Temperature (K)	150	150	150	150
***a*, *b*, *c*, (Å)**	8.64(1), 9.59(1), 16.87(1)	10.50(1), 11.77(1), 12.97(1)	22.06(8), 12.96(1), 10.61(1)	21.67(1), 10.51(1), 12.97(1)
***α*, *β*, *γ*, (°)**	90, 90, 90	92.91(4), 90.58(4), 112.95(4)	90, 90, 90	90, 93.58(4), 90
Z	4	4	8	8
Number of frames	80+130+130	150+150+150+140+233 +150+200+267+150	90+110	333
Continuous rotation (°)	0.50	0.30	0.50	0.30
Resolution (Å^{-1})	1.4	1.4	1.3	1.4
g_{max}, $S_g^{max}(matrix), S_g^{max}(refine)$, R_{Sg}, D_{Sg}	1.4, 0.01, 0.1, 0.7, 0.0015	1.4, 0.01, 0.1 0.66, 0.0015	1.3, 0.01, 0.1, 0.66, 0.0015	1.4, 0.01, 0.1, 0.66, 0.0015
Number of meas./ obs. refl. ($I \geq 3\sigma(I)$)	15213/8545	42023/30910	13667/5161	16734/7084
Number of refined parameters	317	521	158	275
R_{obs} (%), wR_{all} (%), GoF_{obs}	8.88, 9.52, 2.69	13.05, 13.91, 4.00	12.46, 12.90, 3.32	10.12, 11.05, 2.04
Thickness (nm, refined)	119(1), 184(1), 114(1)	90(1), 99(1), 80(1), 136(1), 143(1), 146(1), 159(1), 182(1), 192(1)	101(1), 83(1)	180(1)

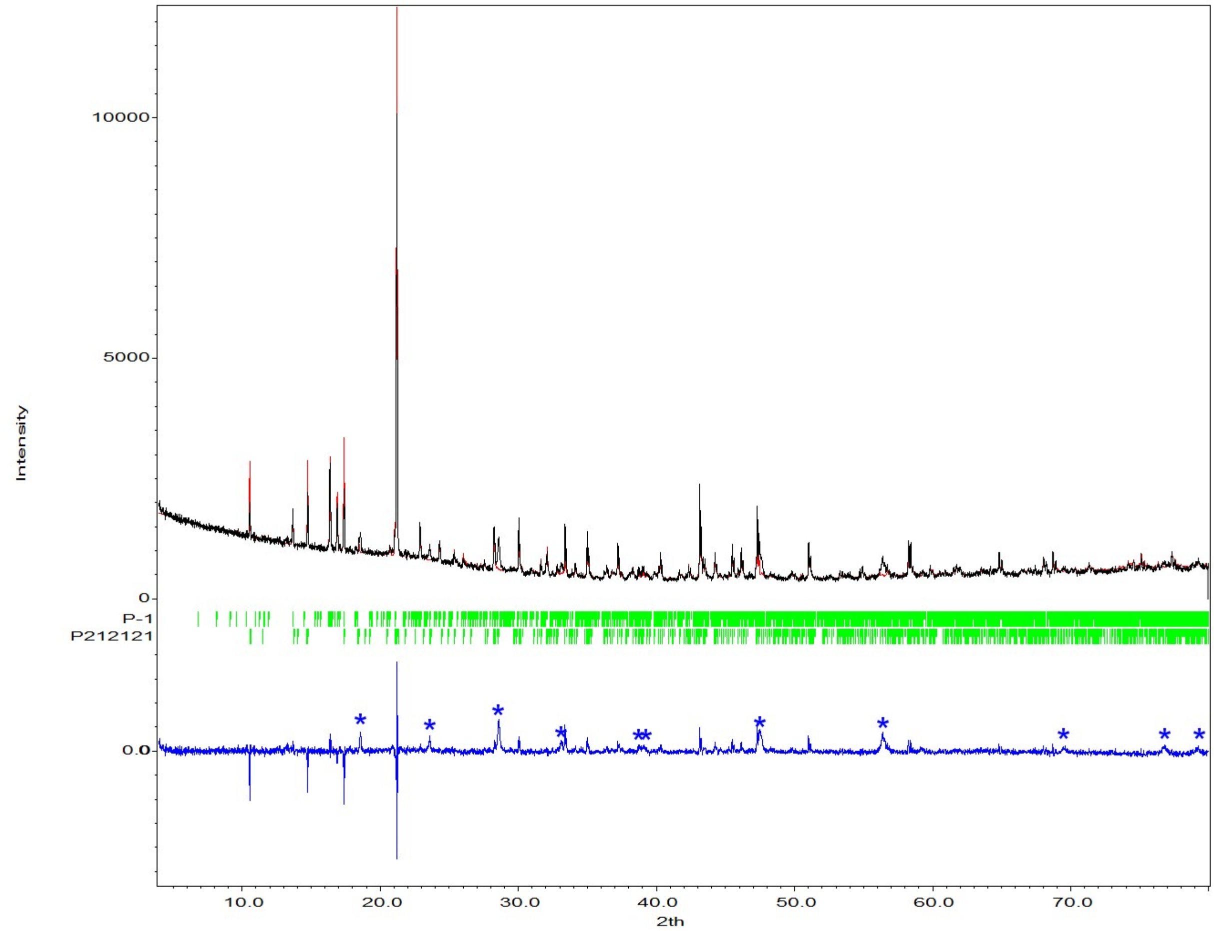

Figure S7 Rietveld refinement of sample treated at 220 °C and 24 hours, pH=7. Data fitted using $P2_12_12_1$ and P-1 structures. The asterisks mark the position of peak, which were not described correctly by the used combination of structure models. The profile of these peaks is much broader than those of the major phases. The increasing profile width with the diffraction angle points to the presence of microstrain in this phase. These extra peaks are very probably due to the minor phases Pbcn or $P2_1/n$, which are rather disordered (significant diffuse scattering observed in 3D ED data) and thus their peak profiles should be broadened.

Figure S8 Bidentate coordination of oxalate to two cerium atoms 1:2 (left), bidentate to two cerium atoms and monodentate to the third cerium atom 1:2+1 (middle), bidentate to three cerium atoms and monodentate to the fourth cerium atom 1:2+2 (right).

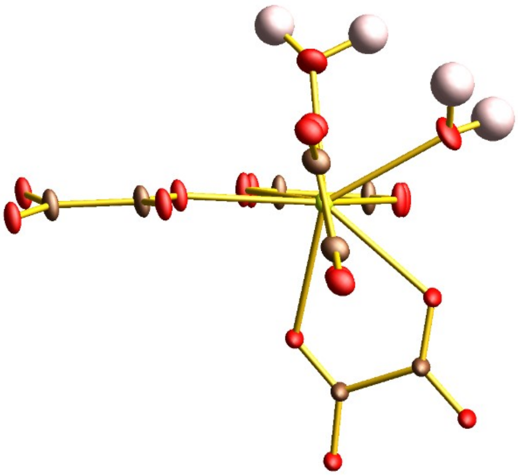

Figure S9 Cerium coordination type 1 viewed along the oxalate infinite chain. Water molecules are in neighbouring positions. Coordination number is nine. One is opposed by bidentate oxalate, and one is opposing monodentate oxalate.

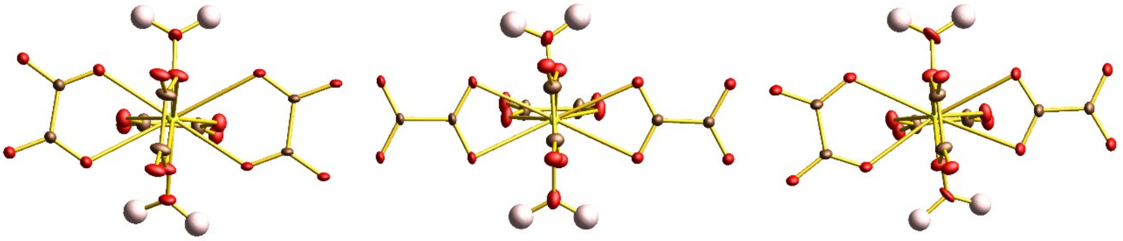

Figure S10 Cerium coordination viewed along the oxalate infinite chain. Water molecules are opposing each other. Coordination number is 10. Type 2 (left) has two bidentate oxalates coordinated by their long side. Type 3 (middle) has two bidentate oxalates coordinated by their short side. Type 4 (right) has two bidentate oxalates, one coordinated by the long side and one coordinated by the short side.

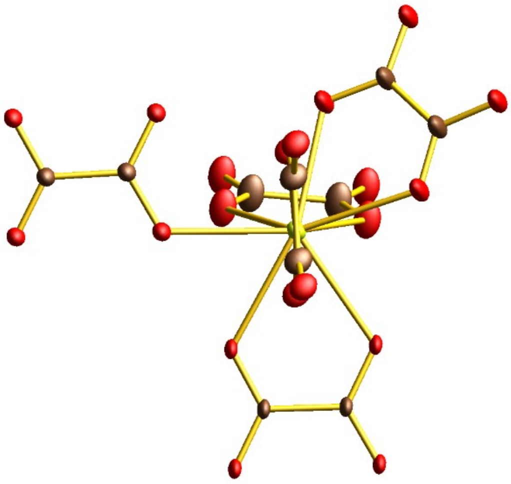

Figure S11 Cerium coordination type 5 viewed along the oxalate infine chain. This cerium is coordinated solely by oxalates. Coordination number is nine and there are four bidentate oxalates and one monodentate.

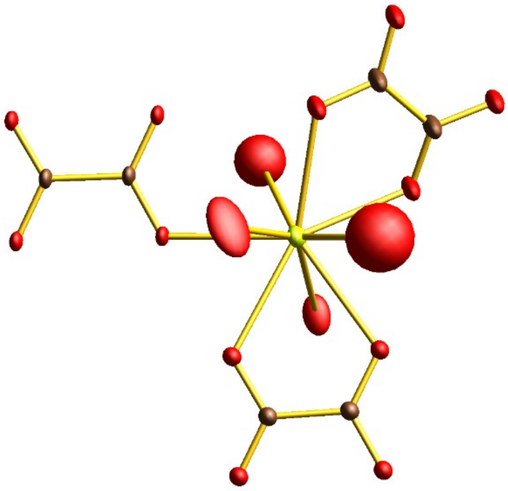

Figure S12 Cerium coordination type 6. This cerium does not contribute to the infinite oxalate chains. Due to steric reasons, it is not possible to interconnect two cerium atoms in the direction of the infinite chains by the oxalates. Instead, there are four coordinated water molecules. There molecules have large displacement parameters. Coordination number is nine and the coordination sphere is completed by two bidentate oxalates and one monodentate.

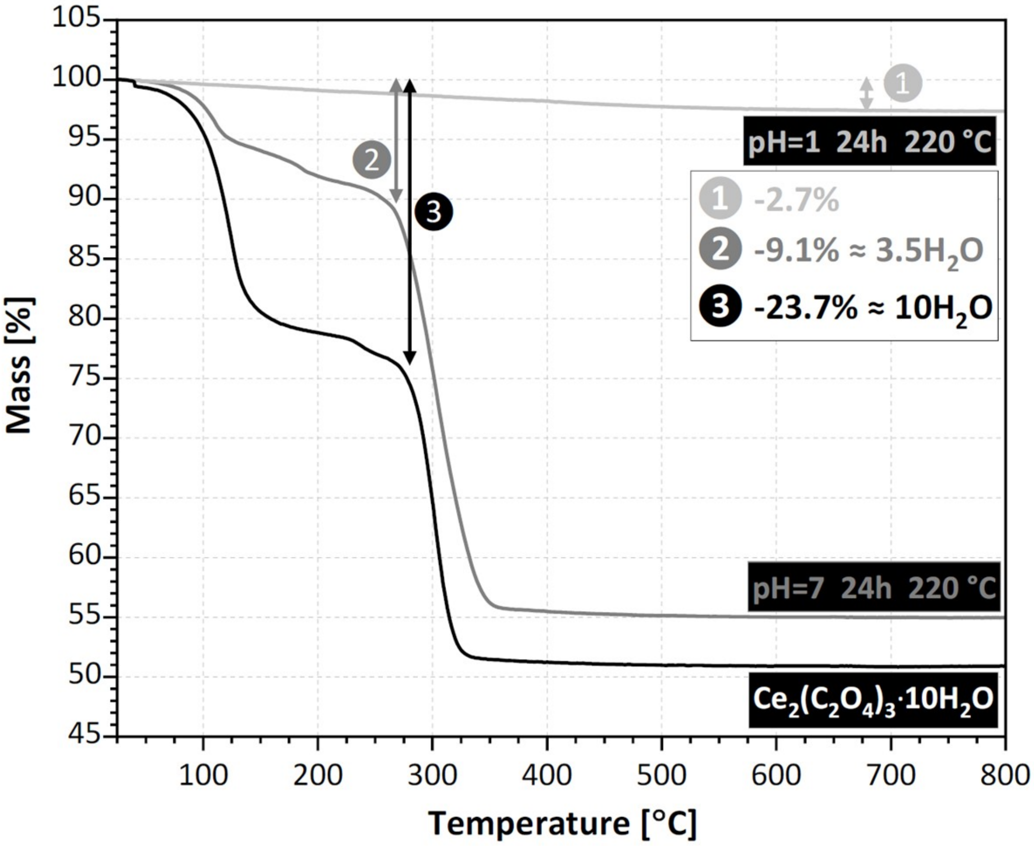

Figure S13 Thermogravimetric measurements of initial cerium oxalate decahydrate, hydrothermally recrystallized oxalate treated at 220 °C, 24 hours and pH=7, and lastly final CeO2 obtained at 220 °C, 24 hours and pH=1.

Discussion of hydration of the sample obtained at 220 °C, 24 hours and pH=7

If we assume all the water molecule occupancies to be full, then except for $P2_12_12_1$, which is tetrahydrate, all the other structures are pentahydrates, where four water molecules are coordinated to the cerium atoms and the fifth resides within the pores of the structures. Data quality and resolution did not allow to refine the occupancies and thus it is not possible to deduce the hydration level directly. However, there exist vast differences in the atomic displacement parameters (ADP) of water molecules coordinated to type 1 and type 2 cerium atoms and ADPs of water molecules coordinated to type 4 (four coordinated water molecules) cerium atoms and water in the pores. The latter group has ADPs much larger than the first one, which may indicate either a positional disorder or a decreased occupancy. The theoretical overall hydration would be 4.5 if we consider the amount of $P2_12_12_1$ and P-1 phases to be equal and we omit the minor phases. The average hydration found by thermogravimetric experiments was about 3.5. In case we admit that the large ADPs of the water coordinated to the type 4 cerium atoms and those found in the pores of the structures is caused by a decreased occupancy of these sites and that the amount of $P2_12_12_1$ and P-1 phases is equal, then the occupancy of the of the sites with the large ADPs should be only 1/3. When we look at the ADPs of the water molecules in the structure P-1, where there are four independent water molecules coordinated to cerium atoms type 2 and six molecules coordinated to type 4 (four molecules) and in the pores (two molecules), the average ADP of the first group is 0.028, while the average ADP within the second group is 0.100, thus more than three times larger than in the first group, which is in line with the hypothesis, that the occupancy of the water molecules coordinated to cerium type 4 and those within the pores is not full.